Arabian Journal of Chemistry 16 (2023) 105290

Contents lists available at ScienceDirect

Arabian Journal of Chemistry

journal homepage: www.sciencedirect.com

Original article

Thermodynamic study for the (butyl, hexyl and octyl) acetoacetate under high pressure CO_2

Hun-Soo Byun *, Pradnya NP Ghoderao, Hyun-Seok Lee, Min-Soo Park

Department of Chemical and Biomolecular Engineering, Chonnam National University, Yeosu, Jeonnam 59626, South Korea

ARTICLE INFO

Article history:
Received 15 May 2023
Accepted 20 September 2023
Available online 25 September 2023

Keywords:
Butyl acetoacetate
High pressure
Hexyl acetoacetate
Octyl acetoacetate
Phase behavior
Supercritical CO_2

ABSTRACT

Understanding the phase behavior of binary liquid mixtures containing butyl acetoacetate, hexyl acetoacetate, and octyl acetoacetate under high-pressure supercritical CO_2 (sc-CO_2) is essential for several applications. The solubility curves for these binary mixtures have been investigated at different temperature and pressure ranges, specifically between 313.2 K and 393.2 K and 2.39 MPa to 23.83 MPa. The three systems, namely butyl acetoacetate, hexyl acetoacetate, and octyl acetoacetate in high-pressure sc-CO_2, exhibit critical mixture curves and a maximum in pressure–temperature (*P, T*) diagrams between the critical point of butyl acetoacetate/hexyl acetoacetate/octyl acetoacetate and carbon dioxide. These characteristics of the critical mixture plot fall under the category of type-I behavior.

The Peng-Robinson equation, which utilizes van der Waals mixing rules and two interaction parameters, is employed to correlate experimental solubility curves and critical mixture curves of the aforementioned three systems. The root mean square deviation percentage (RMSD%) is calculated at each temperature (using temperature-dependent adjusted parameters) for the butyl acetoacetate + sc-CO_2, hexyl acetoacetate + sc-CO_2, and octyl acetoacetate + sc-CO_2 systems, and it ranges from 3.11% to 5.92%, 2.09% to 3.97%, and 1.70% to 3.02%, respectively.

1. Introduction

An environmentally friendly chemical industrial technology that consumes lesser energy and produces fewer toxic residues is highly sought after (Tsoka et al., 2004; Bolm et al., 1999). One promising approach to achieving this is the use of high-pressure processing in combination with supercritical fluids (SCFs). The use of SCFs in chemical industries has been increasing since the early 1980 s due to their sustainability and environmental friendliness (Khalil, 2019; Ramsey et al., 2009; Wagare et al., 2021; Knez et al., 2014). SCFs are becoming increasingly popular as green solvents because they are potentially more affordable, non-toxic, non-flammable, and sustainable than conventional organic solvents that are harmful to the environment (Manjare and Dhingra, 2019; Calvo-Flores et al., 2018). Supercritical fluid technology has a broad scope of applications, such as separation techniques, reaction mediums, synthesis of new materials, powder formation, processing of oils and fats, thin film deposition, and more (Braga et al., 2023; Preetam et al., 2023; Liu et al., 2022; Liang et al., 2023; Agregán et al., 2023; Senyay-Oncel et al., 2023; Tran and Park, 2021; López-Hortas et al., 2022; Li and Xu, 2019; Tsai and Wang, 2019). Butyl, hexyl, and octyl acetoacetates considered in present study are versatile compounds with industrial applications such as flavorings agents and fragrances (Braunschmid et al., 2021; PubChem, n.d.; butyl acetoacetate, n.d.). Hexyl and octyl acetoacetates are used as fuel lubricity additives (Anastopoulos et al., 2001). Hexyl acetoacetate is a chemical with potential uses in polymer formation and antibacterial applications. It can cross-link in polymers, react with other compounds, and exhibits antibacterial activity against E. coli and S. aureus (FH60066, 2023). It is used in the synthesis of various compounds, such as pharmaceuticals, fragrances, and food additives. Hexyl acetoacetates is also used as a solvent in the manufacture of paints, varnishes, and adhesives (Buy Hexyl acetoacetate, 2023). Octyl acetoacetate is a versatile chemical that can serve as a solvent in organic synthesis, a reactant for the synthesis of various compounds, and a reagent in laboratory experiments. Its applications extend to the synthesis of pharmaceuticals, food additives, and fragrances. Furthermore, it can be used as a starting material for polymer synthesis and in the study

* Corresponding author.
E-mail address: hsbyun@jnu.ac.kr (H.-S. Byun).

Peer review under responsibility of King Saud University.

Production and hosting by Elsevier

https://doi.org/10.1016/j.arabjc.2023.105290
1878-5352/

of the effects of different compounds on biochemical and physiological processes in organisms (Buy Octyl acetoacetate, 2023).

Supercritical fluids (SCFs) have the unique ability to solubilized a diverse array of chemicals, making them valuable solvents in various industrial processes. Among the different SCFs, supercritical carbon dioxide (sc-CO_2) is widely used and studied (Yang et al., 2022; Tabernero et al., 2022). Byun's group, has processed several polymers/monomers in sc-CO_2 and analyzed the resulting solubility data (Lee et al., 2023; Ghoderao et al., 2023; Ghoderao et al., 2023; Np Ghoderao et al., 2023). Additionally, another groups have provided experimental phase equilibrium data for various hydrocarbons and sc-CO_2 mixtures (Gao et al., 2021; Gao et al., 2020; Li et al., 2019). Moreover, sc-CO2 has several other applications such as materials processing and synthesis (Zhang et al., 2014), precision cleaning technique (Kohli et al., 2019), microelectronics processing (Giles et al., 1998), hydrotreating, extraction, biomass pretreatment, conversion of waste heat into power, and sterilization of medical equipment (Okolie et al., 2022). High-pressure sc-CO_2 has gained significant attention and importance in separation processes due to its unique properties and several advantages over traditional solvents. Here are some key points highlighting the importance of sc-CO_2 in separation processes and its advantages: 1) *Tunable Properties:* The density and solvation power of sc-CO_2 can be easily tuned by adjusting temperature and pressure, allowing it to be tailored for specific separation tasks. This tunability makes it versatile for a wide range of applications. 2) *Environmentally Friendly:* sc-CO_2 is considered an environmentally friendly solvent because it is non-toxic, non-flammable, and readily available. It does not contribute to environmental pollution, making it a sustainable choice compared to many traditional organic solvents (Dhamodharan et al., 2023). 3) *Low Critical Temperature*: Sc-CO_2 has a relatively low critical temperature and critical pressure, making it suitable for processing temperature-sensitive compounds that may degrade at higher temperatures (Girardi et al., 2023). 4) *Reduced Energy Consumption*: Operating near or above the critical point reduces the energy required for solvent recovery because sc-CO_2 can be easily depressurized and recycled. This can lead to cost savings and improved process efficiency. 5) *Minimized Environmental Impact:* By reducing the use of hazardous organic solvents, sc-CO_2 contributes to reducing the environmental footprint of separation processes, aligning with sustainability and regulatory goals. 6) *Application Diversity*: Sc-CO_2 finds applications in various industries, including pharmaceuticals, food and beverage, cosmetics, petrochemicals, and more. Its versatility and compatibility with different compounds make it a valuable tool for separation processes across different sectors (Balbinot Filho et al., 2023; Sodeifian et al., 2023).

This study has explored the phase behavior of binary mixtures of butyl acetoacetate, hexyl acetoacetate, and octyl acetoacetate with sc-CO_2 using high pressure apparatus. The experimental isotherms for all systems are presented in (*P-x*) space. For the butyl acetoacetate + sc-CO2 system, experimental isotherms (313.2 K $\leq T \leq$ 393.2 K) were obtained in a pressure range of 3.04 MPa $\leq P \leq$ 20.43 MPa, while the pressure and temperature range for hexyl acetoacetate + sc-CO_2 and octyl acetoacetate + sc-CO_2 systems were 2.69 MPa $\leq P \leq$ 22.18 MPa and 2.39 MPa $\leq P \leq$ 23.83 MPa. The critical mixture lines in (P-T) space confirm the type-I behavior exhibited by all binary mixes, meaning that a continuous critical line exists between the sc-CO_2 critical point and the critical point of the other component (butyl acetoacetate or hexyl acetoacetate or octyl acetoacetate) and no liquid–liquid critical line exists.

Another part of this work is to correlate the obtained experimental isotherms with theoretical models. The cubic equations of state are widely used tools to estimate vapor–liquid equilibria and thermodynamic properties (Ghoderao et al., 2018; Ghoderao et al., 2019; Ghoderao et al., 2019; Kristanto et al., 2023). The Peng-Robinson (P-R) equation is a simple cubic equation of state that is accepted and used extensively for various applications (Bhawangirkar et al., 2018; Anil et al., 2022; Avula et al., 2015, 2016, 2017; Joshi et al., 2012). In this study, we have employed the P-R equation utilizing the van der Waals (vdW) mixing rule to predict experimental isotherms. The properties of indiviual pure component such as molecular weight, critical properties, boiling temperature, and acentric factor of carbon dioxide, butyl acetoacetate, hexyl acetoacetate, and octyl acetoacetate are given in Table 1. The pure component properties such as critical temperature, critical pressure, and acentric factor are obtained by Joback–Lyderson group contribution method (Reid et al., 1987). The chemical structures of butyl acetoacetate, hexyl acetoacetate, and octyl acetoacetate are depicted in Fig. 1.

2. Experimental section

2.1. Materials

Tokyo Chemical Industry Co supplied Butyl Acetoacetate (CAS RN 591-60-6), Hexyl Acetoacetate (CAS RN 13562-84-0), and Octyl Acetoacetate (CAS RN 16436-00-3) with purities greater than 0.98, 0.95, and 0.95, respectively. Deok Yang Gases Co supplied pure carbon dioxide with a purity of greater than 0.999. Table 2 presents detailed specifications of the compounds used. All substances were used in their original form.

3. Experimental apparatus and procedure

High-pressure instruments were utilized to measure the phase behavior, as discussed in previous studies (Baek and Byun, 2016). The detailed information regarding the procedures used to obtain the solubility curves in the described experiment as follows:

Equipment: The equipment used for obtaining solubility curves in this study includes:

High-Pressure Equipment (Fig. 2): The primary instrument used to measure phase behavior under high-pressure conditions is detailed below: (1) *Pump Generator*: A pump generator, specifically Model 37–5.75–60 (HIP), is employed in the setup. This pump generator is responsible for generating high-pressure conditions within the system. (2) *Piston and Heise Gauge*: The pump generator is connected to a piston with a diameter of 2.54 cm. The pressure generated by the piston movement is recorded using a Heise gauge, Model CM-53920 (Dresser Ind), with a standard uncertainty of 0.03 MPa. (3) *View Cell:* A flexible volume view cell is a crucial component of the setup. It has specific characteristics, including a volume capacity of 28 cm^3 (inside diameter – 1.59 cm; outside

Table 1
The properties of pure component in carbon dioxide, butyl acetoacetate, hexyl acetoacetate and octyl acetoacetate.

Compounds	M_w	Chemical Structure	T_b / K	T_c / K	p_c / MPa	ω
Carbon Dioxide	44.01	O = C = O		304.2	7.38	0.225
Butyl Acetoacetate	158.20	$C_8H_{14}O_3$	478.2 [a]	653.9	2.72	0.665
Hexyl Acetoacetate	186.25	$C_{10}H_{18}O_3$	512.2[b]	681.2	2.25	0.748
Octyl Acetoacetate	214.30	$C_{12}H_{22}O_3$	531.2–532.2[a]	690.1	1.89	0.819

[a] : The Good Scents Company [b]: Tokyo Chemical Industry Co.

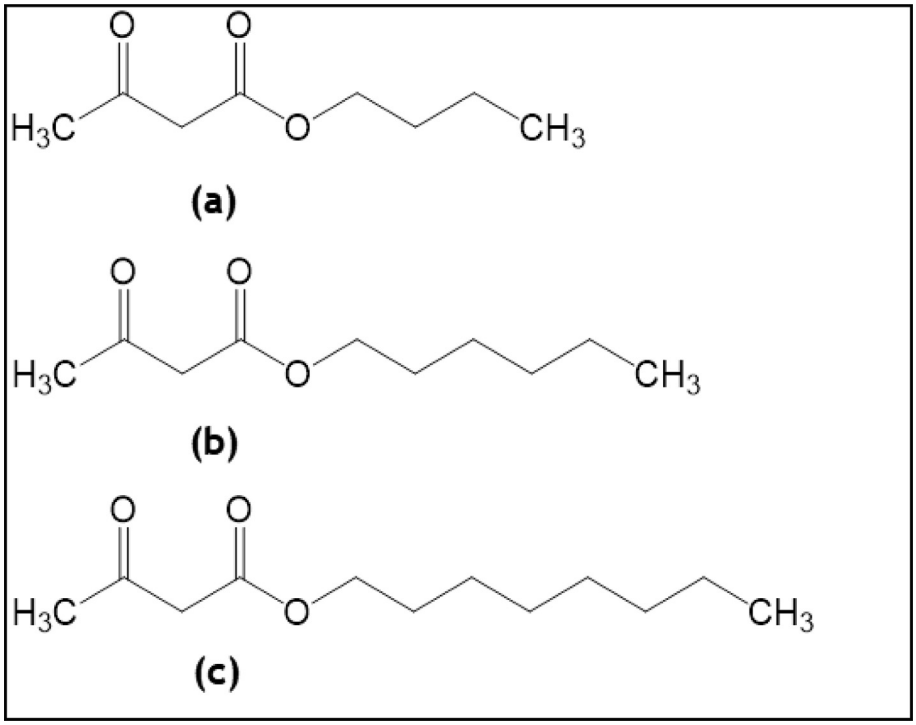

Fig. 1. Chemical structure of (a) butyl acetoacetate (b) hexyl acetoacetate and (c) octyl acetoacetate.

Table 2
Specifications of the chemical used in this work.

Chemical Name	Source	Mass Fraction Purity[a]	Purification Method	Analysis Method[a]
Carbon dioxide	Deok Yang Co.	>0.999	None	–
Butyl acetoacetate	Tokyo Chemical Industry Co.	>0.98	None	GC[b]
Hexyl acetoacetate	Tokyo Chemical Industry Co.	>0.95	None	GC[b]
Octyl acetoacetate	Tokyo Chemical Industry Co.	>0.95	None	GC[b]

[a] Both the analysis method and the mass fraction purity were provided by the suppliers.
[b] Gas-liquid chromatography.

diameter – 6.4 cm). This view cell is designed to withstand pressures up to 70 MPa. (4) *Transparent Glass Window:* To enable the observation of mixture phase transitions, a transparent glass window is attached to the front portion of the view cell. This window has a thickness of 1.9 cm and a diameter of 1.9 cm. (5) *Camera and Monitor*: A video monitor is used in conjunction with a camera connected to an Olympus Corp borescope (Model - F100-038–000-50) positioned against the glass window to observe the mixture.

The procedure for obtaining solubility curves involves the following steps: (1) *Initial Purging*: To eliminate any residual air and organic materials, the view cell is initially purged with nitrogen (N_2) and sc-CO_2. Sc-CO_2 is introduced into the view cell using a pressure bomb with an uncertainty of 0.002 g. (2) *Mixture Preparation*: A specimen of the binary mixture is prepared and inserted into the view cell using a syringe with an uncertainty of 0.0002 g. The precise composition of this mixture is determined based on the experimental objectives. (3) *Pressurization and Equilibration*: The binary mixture in the view cell is pressurized and maintained at a constant phase for a duration of thirty minutes. This is achieved by regulating the piston to attain the desired pressure level and temperature, which are then held constant. After thirty minutes, it is assumed that phase equilibrium has been achieved inside the cell. (4) *Solubility Measurement*: The pressure is gradually decreased to observe different phases. The appearance of small bubbles or a fine mist inside the view cell with varying pressure is recorded as a bubble point (I) or dew point (III), respectively. The critical point (II) of the mixture is noted when opalescence is observed with equal gas and liquid volume. (5) *Repetition*: Each measurement is repeated at least three times to ensure accuracy and reproducibility.

4. Results and discussion

The article presents an investigation into the binary systems of sc-CO_2 with butyl acetoacetate, hexyl acetoacetate, and octyl acetoacetate. The study reports the isotherms in (P, x) space, where P denotes pressure and $\times$ signifies mole fraction. The standard uncertainties (σ) associated with the measurement of pressure, temperature, and mole fraction were found to be σ (P): 0.2 MPa, σ (T): 0.2 K, and σ (x): 0.0008, respectively. The experimental isotherms of the sc-CO_2 + butyl acetoacetate binary system were reported in Table 3 for the pressure range of 3.04 MPa to 20.43 MPa and temperature array of 313.2 K to 393.2 K. The phase equilibrium behaviour of the sc-CO_2 + hexyl acetoacetate solution was shown in Table 4 for the pressure range of 2.69 MPa to 22.18 MPa and temperature array of 313.2 K to 393.2 K. Similarly, the phase characteristics of the sc-CO_2 + octyl acetoacetate system were demonstrated in Table 5 for the pressure range of 2.39 MPa to 23.83 MPa and temperature range of 313.2 K to 393.2 K.

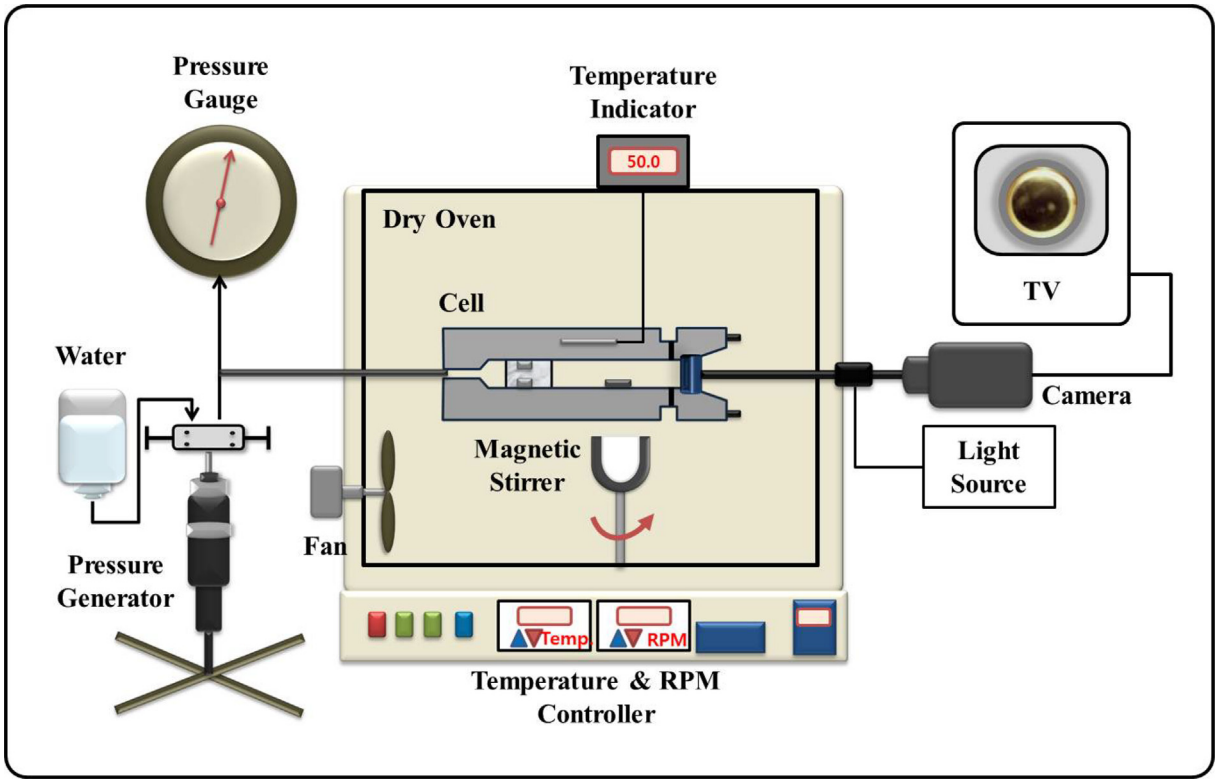

Fig. 2. Schematic diagram of high-pressure apparatus.

Fig. 3 (a-c) in this study compare experimental isotherms with computed isotherms using the P-R equation for the sc-CO_2 + butyl acetoacetate, sc-CO_2 + hexyl acetoacetate, and Sc-CO_2 + octyl acetoacetate mixtures at a temperature of 353.2 K. T = 353.2 K is an intermediate temperature in the range of temperatures measured. The experimental results indicate that a vapor–liquid equilibrium region is observed beneath each isotherm, while a single-phase region is reported above every isotherm. Furthermore, no three-phase region was detected at any of the five temperatures that were investigated. The fitted interaction two-parameters (ITPs) for the 353.2 K isotherm are shown as a red solid line, with k_{ij} and η_{ij} values of 0.015 and −0.055 for butyl acetoacetate + sc-CO_2 (using 14 data points), 0.020 and −0.040 for hexyl acetoacetate + sc-CO_2 (using 14 data points), and 0.050 and −0.025 for octyl acetoacetate + sc-CO_2 (using 14 data points). In contrast, the results with ITPs set to zero (k_{ij} = 0.0 and η_{ij} = 0.0) are shown as a solid blue line. The RMSD% (root mean square relative deviation percentage) was calculated at 353.2 K for each system, and the values were 3.24%, 2.09%, and 1.70% for butyl acetoacetate + sc-CO_2, hexyl acetoacetate + sc-CO_2, and octyl acetoacetate + sc-CO_2, respectively. The figures clearly show that the isotherms predicted with zero ITPs significantly deviate from the experimental values. Therefore, the other isotherms were calculated using non-zero ITPs. It is important to note that the ITPs calculated for the 353.2 K isotherms were used to calculate the other isotherms in present case.

The van der Waals mixing rules with ITPs are as given below:

$$a_{mix} = \sum_i \sum_i x_i x_j a_{ij} \tag{1}$$

$$b_{mix} = \sum_i \sum_i x_i x_j b_{ij} \tag{2}$$

$$a_{ij} = (a_{ii} a_{jj})^{\frac{1}{2}} (1 - \kappa_{ij}) \tag{3}$$

$$b_{ij} = \frac{1}{2}(b_{ii} + b_{jj})(1 - \eta_{ij}) \tag{4}$$

The optimization of the objective function in equation (5) to obtain ITPs was carried out using the least square method in Python programming.

$$OB = \sum_{i=1}^{N} \left(\frac{P_{exp} - P_{cal}}{P_{exp}} \right) \tag{5}$$

where P_{exp} is experimental pressure, P_{cal} is calculated pressure, and N are number of data points. The RMSD% is calculated for assessment of accuracy in the prediction of bubble pressure for different isotherms. The RMSD % is given as,

$$RMSD\,\% = \sqrt{\frac{OB}{N}} \times 100 \tag{6}$$

where, OB is the objective function in eq. (5) and N are number of data points.

The ITPs obtained in studies of binary mixtures have significant physical significance and are related to the molecular interactions occurring within these mixtures. These parameters are often used to describe and understand the non-ideal behavior of binary systems, where the interactions between molecules are not simply additive. Here's the physical significance of these parameters and their relation to molecular interactions: (1) *Deviation from Ideal Behavior:* Binary interaction parameters, often denoted as binary interaction coefficients (e.g., k_{ij} or η_{ij}), quantify the deviation of a binary mixture from ideal behavior. Ideal behavior assumes that the mixture's properties can be calculated as weighted averages of the pure component properties. When the binary interaction parameter is zero (k_{ij} = 0), the mixture follows ideal behavior. Positive or negative values of kij indicate deviations from ideality. (2) *Attractive and Repulsive Interactions*: The sign of the binary interaction parameter indicates the nature of molecular interactions between the components. Positive k_{ij}: Indicates repulsive interac-

Table 3
Experimental data for the (sc-CO_2 + butyl acetoacetate) {(1 - x) sc-CO_2 + x $C_8H_{14}O_3$} system in this work.

Butyl Acetoacetate Mole Fraction	p[a] / MPa	Transition[b] and Phase[c]
T[a] / K = 313.2		
0.0450	8.62	I (L → LV)
0.0661	8.68	I (L → LV)
0.0756	8.69	I (L → LV)
0.0968	8.62	I (L → LV)
0.1068	8.55	I (L → LV)
0.1196	8.50	I (L → LV)
0.1576	8.28	I (L → LV)
0.2142	7.92	I (L → LV)
0.3110	7.31	I (L → LV)
0.4271	6.41	I (L → LV)
0.5180	5.51	I (L → LV)
0.6116	4.72	I (L → LV)
0.7545	3.55	I (L → LV)
0.8239	3.04	I (L → LV)
T / K = 333.2		
0.0450	12.03	III(V → VL)
0.0661	12.12	I (L → LV)
0.0756	12.03	I (L → LV)
0.0968	11.83	I (L → LV)
0.1068	11.72	I (L → LV)
0.1196	11.48	I (L → LV)
0.1576	11.03	I (L → LV)
0.2142	10.40	I (L → LV)
0.3110	9.18	I (L → LV)
0.4271	7.94	I (L → LV)
0.5180	6.69	I (L → LV)
0.6116	5.76	I (L → LV)
0.7545	4.07	I (L → LV)
0.8239	3.36	I (L → LV)
T / K = 353.2		
0.0450	15.21	III(V → VL)
0.0661	15.33	II(LV)
0.0756	15.27	I (L → LV)
0.0968	15.04	I (L → LV)
0.1068	14.79	I (L → LV)
0.1196	14.55	I (L → LV)
0.1576	14.04	I (L → LV)
0.2142	13.04	I (L → LV)
0.3110	11.10	I (L → LV)
0.4271	9.42	I (L → LV)
0.5180	7.79	I (L → LV)
0.6116	6.76	I (L → LV)
0.7545	4.35	I (L → LV)
0.8239	3.66	I (L → LV)
T / K = 373.2		
0.0450	17.86	III(V → VL)
0.0661	18.14	III(V → VL)
0.0756	18.21	II(LV)
0.0968	18.06	I (L → LV)
0.1068	17.96	I (L → LV)
0.1196	17.75	I (L → LV)
0.1576	17.07	I (L → LV)
0.2142	15.68	I (L → LV)
0.3110	13.37	I (L → LV)
0.4271	11.24	I (L → LV)
0.5180	8.86	I (L → LV)
0.6116	7.48	I (L → LV)
0.7545	4.55	I (L → LV)
0.8239	3.90	I (L → LV)
T / K = 393.2		
0.0450	19.55	III(V → VL)
0.0661	20.24	III(V → VL)
0.0756	20.43	III(V → VL)
0.0968	20.37	I (L → LV)
0.1068	20.34	I (L → LV)
0.1196	20.21	I (L → LV)
0.1576	19.73	I (L → LV)
0.2142	17.93	I (L → LV)
0.3110	15.33	I (L → LV)
0.4271	12.41	I (L → LV)
0.5180	10.14	I (L → LV)
0.6116	8.07	I (L → LV)
0.7545	4.83	I (L → LV)
0.8239	4.04	I (L → LV)

[a] Standard uncertainties σ are $\sigma(T)$ = 0.2 K, $\sigma(p)$ = 0.2 MPa and $\sigma(x)$ = 0.0008.
[b] I: Bubble-point, II: Critical-point, III: Dew-point, [c]L: Liquid phase, V: Gas phase.

Table 4
Experimental data for the (sc-CO_2 + hexyl acetoacetate) {(1 - x) sc-CO_2 + x $C_{10}H_{18}O_3$} system in this work.

Hexyl Acetoacetate Mole Fraction	p[a] / MPa	Transition[b] and Phase[c]
T[a] / K = 313.2		
0.0548	8.76	I (L → LV)
0.0690	8.72	I (L → LV)
0.0980	8.66	I (L → LV)
0.1222	8.49	I (L → LV)
0.1418	8.39	I (L → LV)
0.1875	7.99	I (L → LV)
0.2497	7.42	I (L → LV)
0.3297	6.77	I (L → LV)
0.4030	6.21	I (L → LV)
0.4797	5.42	I (L → LV)
0.5472	4.90	I (L → LV)
0.6545	3.98	I (L → LV)
0.6815	3.63	I (L → LV)
0.7620	2.69	I (L → LV)
T / K = 333.2		
0.0548	12.56	I (L → LV)
0.0690	12.45	I (L → LV)
0.0980	12.26	I (L → LV)
0.1222	11.89	I (L → LV)
0.1418	11.59	I (L → LV)
0.1875	11.10	I (L → LV)
0.2497	10.09	I (L → LV)
0.3297	8.88	I (L → LV)
0.4030	7.91	I (L → LV)
0.4797	6.90	I (L → LV)
0.5472	6.07	I (L → LV)
0.6545	4.87	I (L → LV)
0.6815	4.52	I (L → LV)
0.7620	3.17	I (L → LV)
T / K = 353.2		
0.0548	15.97	III(V → VL)
0.0690	16.17	II(LV)
0.0980	16.04	I (L → LV)
0.1222	15.52	I (L → LV)
0.1418	14.97	I (L → LV)
0.1875	13.73	I (L → LV)
0.2497	12.67	I (L → LV)
0.3297	11.00	I (L → LV)
0.4030	9.59	I (L → LV)
0.4797	8.35	I (L → LV)
0.5472	7.10	I (L → LV)
0.6545	5.63	I (L → LV)
0.6815	5.17	I (L → LV)
0.7620	3.68	I (L → LV)
T / K = 373.2		
0.0548	19.32	III(V → VL)
0.0690	19.41	III(V → VL)
0.0980	19.29	I (L → LV)
0.1222	19.03	I (L → LV)
0.1418	18.45	I (L → LV)
0.1875	17.29	I (L → LV)

(continued on next page)

Table 4 (*continued*)

Hexyl Acetoacetate Mole Fraction	p^a / MPa	Transition[b] and Phase[c]
0.2497	15.66	I (L → LV)
0.3297	13.31	I (L → LV)
0.4030	11.10	I (L → LV)
0.4797	9.52	I (L → LV)
0.5472	7.96	I (L → LV)
0.6545	6.28	I (L → LV)
0.6815	5.66	I (L → LV)
0.7620	4.05	I (L → LV)
T / K = 393.2		
0.0548	21.86	III(V → VL)
0.0690	22.18	III(V → VL)
0.0980	21.97	I (L → LV)
0.1222	21.52	I (L → LV)
0.1418	20.93	I (L → LV)
0.1875	19.91	I (L → LV)
0.2497	17.92	I (L → LV)
0.3297	15.31	I (L → LV)
0.4030	12.85	I (L → LV)
0.4797	11.03	I (L → LV)
0.5472	9.21	I (L → LV)
0.6545	6.90	I (L → LV)
0.6815	6.10	I (L → LV)
0.7620	4.15	I (L → LV)

[a] Standard uncertainties σ are $\sigma(T)$ = 0.2 K, $\sigma(p)$ = 0.2 MPa and $\sigma(x)$ = 0.0008.
[b] I: Bubble-point, II: Critical-point, III: Dew-point, [c]L: Liquid phase, V: Gas phase.

Table 5
Experimental data for the (sc-CO_2 + octyl acetoacetate) {(1 - *x*) sc-CO_2 + *x* $C_{12}H_{22}O_3$} system in this work.

Octyl Acetoacetate Mole Fraction	p^a / MPa	Transition[b] and Phase[c]
T^a / K = 313.2		
0.0405	9.38	I (L → LV)
0.0750	9.45	I (L → LV)
0.0784	9.38	I (L → LV)
0.1039	9.30	I (L → LV)
0.1253	9.17	I (L → LV)
0.1540	8.86	I (L → LV)
0.1755	8.72	I (L → LV)
0.2897	7.49	I (L → LV)
0.3540	6.94	I (L → LV)
0.4010	6.43	I (L → LV)
0.5154	5.14	I (L → LV)
0.6176	4.07	I (L → LV)
0.7221	3.08	I (L → LV)
0.7948	2.39	I (L → LV)
T / K = 333.2		
0.0405	13.76	III(V → VL)
0.0750	13.80	I (L → LV)
0.0784	13.87	I (L → LV)
0.1039	13.59	I (L → LV)
0.1253	13.08	I (L → LV)
0.1540	12.41	I (L → LV)
0.1755	12.18	I (L → LV)
0.2897	10.21	I (L → LV)
0.3540	9.28	I (L → LV)
0.4010	8.46	I (L → LV)
0.5154	6.44	I (L → LV)
0.6176	5.18	I (L → LV)
0.7221	3.80	I (L → LV)
0.7948	2.90	I (L → LV)
T / K = 353.2		
0.0405	17.86	III(V → VL)
0.0750	18.06	II(VL)
0.0784	18.03	I (L → LV)
0.1039	17.48	I (L → LV)
0.1253	17.22	I (L → LV)

Table 5 (*continued*)

Octyl Acetoacetate Mole Fraction	p^a / MPa	Transition[b] and Phase[c]
0.1540	16.48	I (L → LV)
0.1755	15.90	I (L → LV)
0.2897	12.52	I (L → LV)
0.3540	11.28	I (L → LV)
0.4010	10.06	I (L → LV)
0.5154	7.68	I (L → LV)
0.6176	6.06	I (L → LV)
0.7221	4.43	I (L → LV)
0.7948	3.20	I (L → LV)
T / K = 373.2		
0.0405	20.90	III(V → VL)
0.0750	21.24	III(V → VL)
0.0784	21.35	I (L → LV)
0.1039	20.83	I (L → LV)
0.1253	20.43	I (L → LV)
0.1540	19.90	I (L → LV)
0.1755	19.32	I (L → LV)
0.2897	15.17	I (L → LV)
0.3540	13.52	I (L → LV)
0.4010	11.48	I (L → LV)
0.5154	8.78	I (L → LV)
0.6176	6.75	I (L → LV)
0.7221	4.88	I (L → LV)
0.7948	3.51	I (L → LV)
T / K = 393.2		
0.0405	23.32	III(V → VL)
0.0750	23.73	III(V → VL)
0.0784	23.83	II(VL)
0.1039	23.48	I (L → LV)
0.1253	23.18	I (L → LV)
0.1540	22.39	I (L → LV)
0.1755	21.77	I (L → LV)
0.2897	17.17	I (L → LV)
0.3540	15.31	I (L → LV)
0.4010	13.33	I (L → LV)
0.5154	10.11	I (L → LV)
0.6176	7.64	I (L → LV)
0.7221	5.72	I (L → LV)
0.7948	3.85	I (L → LV)

[a] Standard uncertainties σ are $\sigma(T)$ = 0.2 K, $\sigma(p)$ = 0.2 MPa and $\sigma(x)$ = 0.0008.
[b] I: Bubble-point, II: Critical-point, III: Dew-point.
[c] L: Liquid phase, V: Gas phase.

tions between molecules. In such mixtures, the molecules tend to avoid each other, a positive deviation from Raoult's law. *Negative* k_{ij}: Suggests attractive interactions between molecules. In these mixtures, molecules tend to be more attracted to each other, which can lead to a negative deviation from Raoult's law.

Fig. 4 **(a)** presents evaluating agreement between the empirical measurements data and the predicted values using (*P*, *x*) data for the sc-CO_2 + butyl acetoacetate solution. To obtain solubility isotherms, the k_{ij} and η_{ij} values are optimized for each temperature spanned from 313.2 K to 393.2 K. The vapor + liquid equilibria data determined in this study was in good agreement and fitted well into the P-R equation for the sc-CO_2 + butyl acetoacetate mixture. The RMSD% (Table 6) of the sc-CO_2 + butyl acetoacetate solution was calculated for five different temperatures using the two parameters (k_{ij}, η_{ij}) obtained at each temperature.

Fig. 4 **(b)** shows the experimental and calculated curves obtained from the P-R equation using the optimized two parameters obtained at each temperature for the sc-CO_2 + hexyl acetoacetate solution. In this study, we evaluated the RMSDs at five different temperatures varied between (313.2 K to 393.2 K, interval 20 K) for the sc-CO_2 + hexyl acetoacetate solution using the P-R equation with optimized two parameters (Table 6).

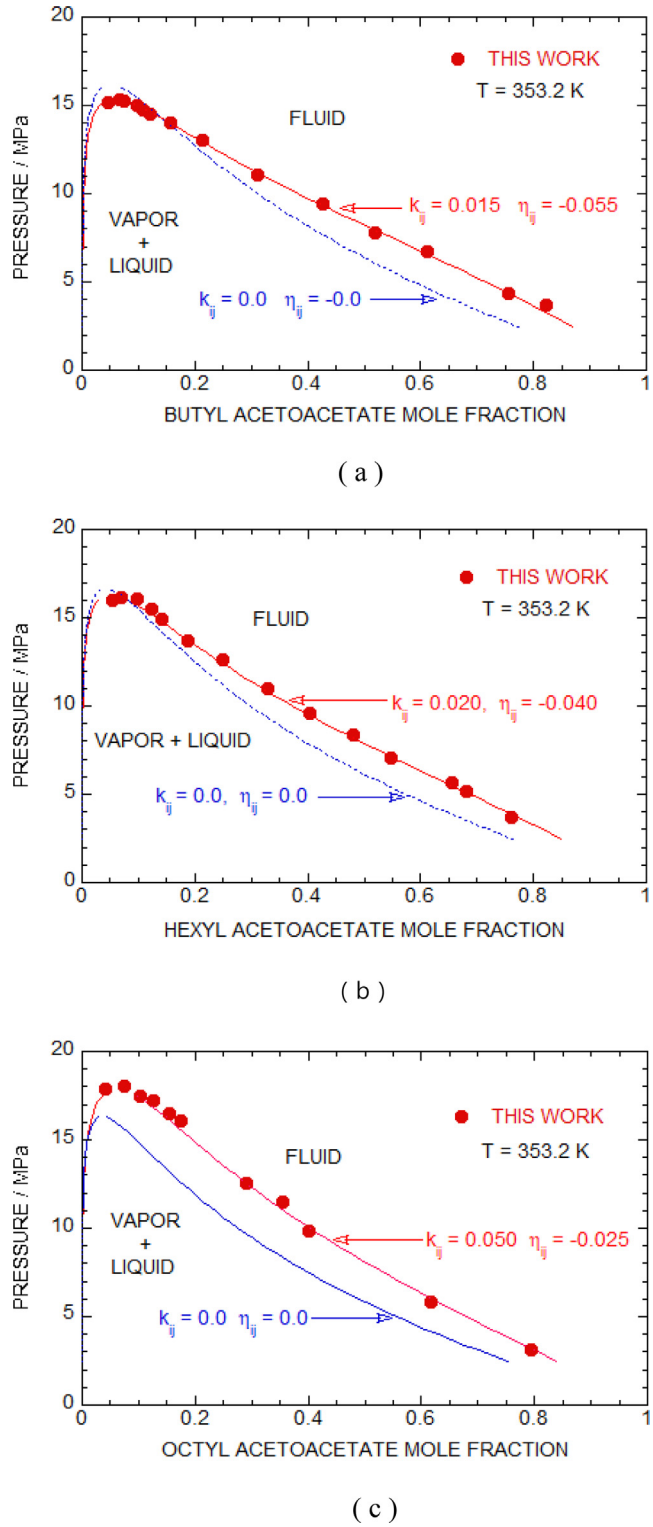

Fig. 3. Pressure vs mole fraction plot (a) butyl acetoacetate + sc-CO_2 (b) hexyl acetoacetate + sc-CO_2 and (c) octyl acetoacetate + sc-CO_2 systems with calculations obtained from PR EOS at 353.2 K. Blue broken and red solid line represent results with zero and non-zero interaction parameters (k_{ij} and η_{ij}) respectively.

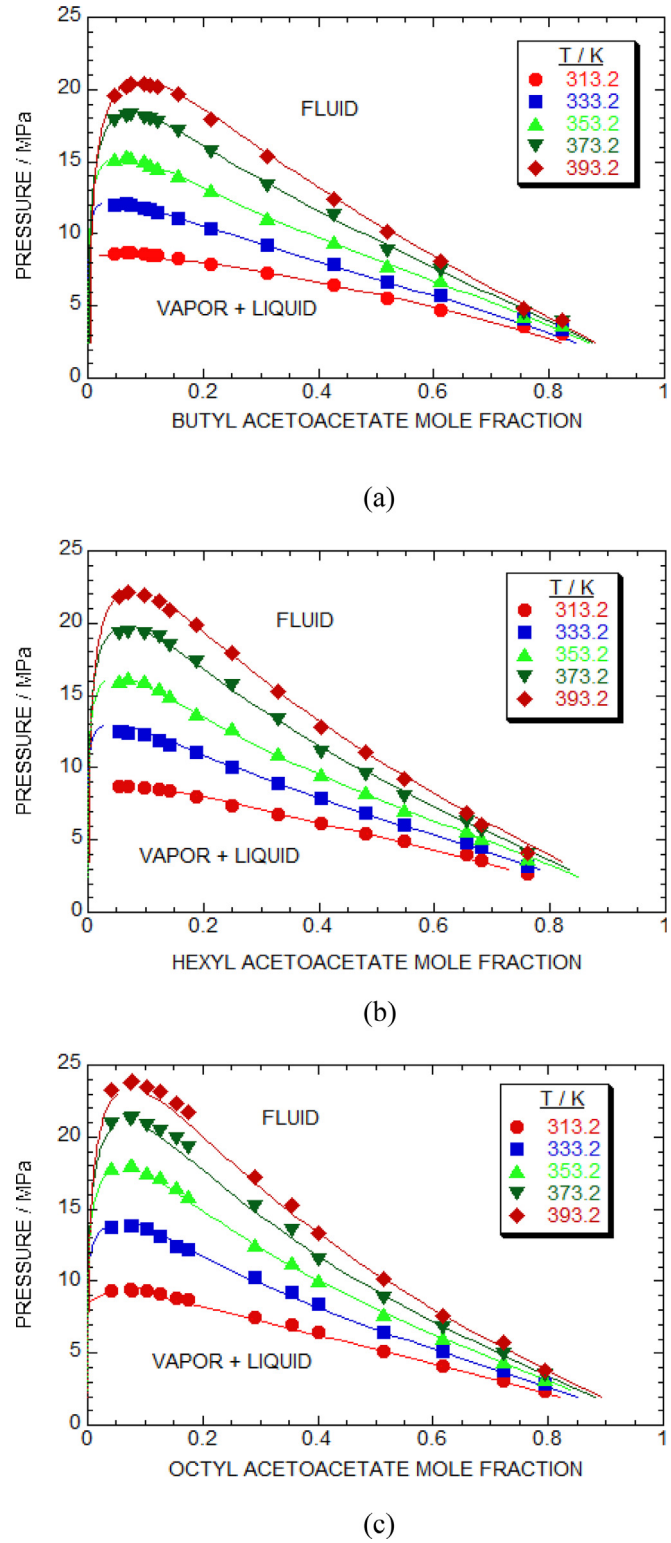

Fig. 4. Experimental and predicted isotherms of (a) butyl acetoacetate + sc-CO_2 (b) hexyl acetoacetate + sc-CO_2 and (c) octyl acetoacetate + sc-CO_2 systems by optimum parameters (k_{ij}, η_{ij}) at each temperature. Symbols denotes experimental data points at various temperature. Solid lines are predicted isotherms using PR EOS.

Fig. 4 **(c)** depicts a comparison between the equilibria data and the estimated results of the (P, x) isotherms at temperatures ranging from 313.2 K to 393.2 K for the sc-CO_2 + octyl acetoacetate system. The adjusted k_{ij} and η_{ij} values (Table 6) were obtained at each temperature, which were 0.058 and −0.028 for T = 313.2 K, 0.054 and −0.026 for T = 333.2 K, 0.050 and −0.025 for T = 353.2 K, 0.048 and −0.020 for T = 373.2 K, and 0.046 and −0.018 for T = 393.2 K.

Table 6
Two interaction parameters (k_{ij} and η_{ij}) and RMSD % for the sc-CO_2 + butyl acetoacetate, sc-CO_2 + hexyl acetoacetate and sc-CO_2 + octyl acetoacetate systems.

Systems	T / K	k_{ij}	η_{ij}	RMSD(%)
SC-CO2 + Butyl acetoacetate	313.2	0.055	−0.045	5.92
	333.2	0.030	−0.050	5.07
	353.2	0.015	−0.055	3.24
	373.2	0.015	−0.045	3.39
	393.2	0.015	−0.035	3.11
SC-CO2 + Hexyl acetoacetate	313.2	0.050	−0.030	2.44
	333.2	0.035	−0.035	2.72
	353.2	0.020	−0.040	2.09
	373.2	0.025	−0.030	2.30
	393.2	0.025	−0.025	3.97
SC-CO2 + Octyl acetoacetate	313.2	0.058	−0.028	2.29
	333.2	0.054	−0.026	2.57
	353.2	0.050	−0.025	1.70
	373.2	0.048	−0.020	2.53
	393.2	0.046	−0.018	3.02

In Fig. 5 **(a-c)**, mixture critical curves of experimental data were compared with the predicted results from the P-R equation for the sc-CO_2 + butyl acetoacetate (a), sc-CO_2 + hexyl acetoacetate (b) and sc-CO_2 + octyl acetoacetate (c) solutions. The projected mixture-critical lines showed a type-I curve, as mentioned before. The red solid lines represented the saturated vapor pressure for individual pure sc-CO_2, butyl acetoacetate, hexyl acetoacetate, and octyl acetoacetate estimated by the Lee-Kesler method (Poling et al., 2001). The red closed circles represented the critical-point for pure sc-CO_2, butyl acetoacetate, hexyl acetoacetate and octyl acetoacetate. Region above the blue dashed curves is in the 1-phase, while below part is in the 2-phase. The dashed curve represented the calculated results determined by the P-R equation, with k_{ij} and η_{ij} values of 0.015 and −0.055 (for butyl acetoacetate), 0.020 and −0.040 (for hexyl acetoacetate), and 0.050 and −0.025 (for octyl acetoacetate). The blue closed squares represented the mixture-critical point obtained from the isotherms measured in the experiment.

5. Conclusion

The equilibrium data of the sc-CO_2 + butyl acetoacetate, sc-CO_2 + hexyl acetoacetate, and sc-CO_2 + octyl acetoacetate systems were obtained at pressures of $P \leq 23.83$ MPa and temperatures extending from 313.2 K to 393.2 K. It was observed that the binary mixtures of sc-CO_2 + butyl acetoacetate, sc-CO_2 + hexyl acetoacetate, and sc-CO_2 + octyl acetoacetate exhibited type-I curves and did not display a three-phase region.

To model the experimental equilibria data from the sc-CO_2 + butyl acetoacetate, sc-CO2 + hexyl acetoacetate, and sc-CO_2 + octyl acetoacetate solutions, the P-R equation was used with adjustable temperature dependent two-parameters, k_{ij} and η_{ij}. The overall RMSD% values for the sc-CO_2 + butyl acetoacetate, sc-CO_2 + hexyl acetoacetate, and sc-CO_2 + octyl acetoacetate solutions were found to be 4.15 %, 2.7 %, and 2.42 %, respectively. These findings suggest that the P-R equation with adjustable two-parameters (k_{ij} and η_{ij}) can effectively model the equilibrium data of the sc-CO_2 + butyl acetoacetate, sc-CO_2 + hexyl acetoacetate, and sc-CO_2 + octyl acetoacetate systems.

The experimental findings and successful application of the Peng-Robinson equation with adjustable parameters (k_{ij} and η_{ij}) to model equilibrium data for sc-CO_2 with various acetoacetate compounds have significant practical implications for process design and optimization in separation processes. This research provides valuable insights into the phase behavior of these systems, aiding in the development of selective extraction processes, optimizing temperature and pressure conditions, and potentially reducing the environmental impact through the use of environmentally friendly sc-CO_2 as a solvent. Additionally, the modeling approach's success suggests its applicability to industrial-scale processes, promising more efficient and sustainable separation techniques across industries.

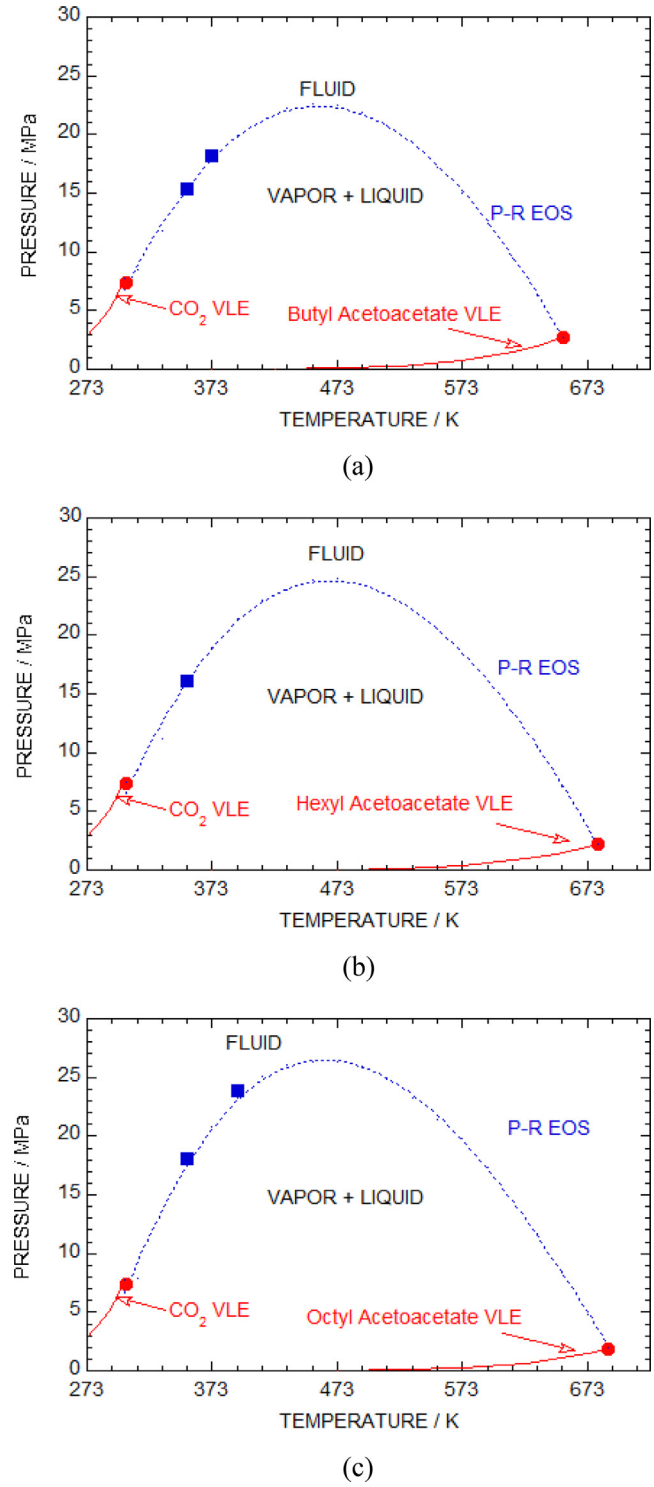

Fig. 5. Diagram in (P vs T) space for the (a) butyl acetoacetate + sc-CO_2 (b) hexyl acetoacetate + sc-CO_2 and (c) octyl acetoacetate + sc-CO_2 systems. The critical-point of pure components (sc-CO_2 or butyl acetoacetate or hexyl acetoacetate or octyl acetoacetate) is represented by red closed circles. Red solid curves are vapor + liquid equilibrium curves. Squares denotes critical points of a mixture taken from experimental isotherms. Black and blue curves show calculations by P-R equation with zero and non-zero interaction parameters.

CRediT authorship contribution statement

Hun-Soo Byun: Conceptualization, Validation, Visualization, Supervision, Project administration, Funding acquisition, Writing – original draft. **Pradnya NP Ghoderao:** Conceptualization, Methodology, Formal analysis, Data curation, Software, Investigation. **Hyun-Seok Lee:** Methodology, Data curation, Investigation. **Min-Soo Park:** Methodology, Data curation, Investigation.

Declaration of competing interest

The authors declare that they have no known competing financial interests or personal relationships that could have appeared to influence the work reported in this paper.

Acknowledgements

This work was supported by the National Research Foundation of Korea (NRF) grant funded by the Korea government (MSIT) (No. 2021R1A2C2006888).

References

Agregán, R., Bangar, S.P., Hassoun, A., Hano, C., Pateiro, M., Lorenzo, J.M., 2023. Green technologies for sustainable food production and preservation: supercritical fluids. In: Reference Module in Food Science. Elsevier. https://doi.org/10.1016/B978-0-12-823960-5.00078-0.

Anastopoulos, G., Lois, E., Zannikos, F., Kalligeros, S., Teas, C., 2001. Influence of aceto acetic esters and di-carboxylic acid esters on diesel fuel lubricity. Tribol. Int. 34, 749–755. https://doi.org/10.1016/S0301-679X(01)00067-6.

Anil, J.N., Bhawangirkar, D.R., Sangwai, J.S., 2022. Effect of guest-dependent reference hydrate vapor pressure in thermodynamic modeling of gas hydrate phase equilibria, with various combinations of equations of state and activity coefficient models. Fluid Phase Equilib. 556, 113356.

Avula, V.R., Gardas, R.L., Sangwai, J.S., 2015. An efficient model for the prediction of CO2 hydrate phase stability conditions in the presence of inhibitors and their mixtures. J. Chem. Thermodyn. 85, 163–170.

Avula, V.R., Gardas, R.L., Sangwai, J.S., 2016. A robust model for the phase stability of clathrate hydrate of methane in an aqueous systems of TBAB, TBAB þ NaCl and THF suitable for storage and transportation of natural gas. J. Nat. Gas Sci. Eng. 33, 509–517.

Avula, V.R., Gupta, P., Gardas, R.L., Sangwai, J.S., 2017. Thermodynamic modeling of phase equilibrium of carbon dioxide clathrate hydrate in aqueous solutions of promoters and inhibitors suitable for gas separation. Asia-Pac. J. Chem. Eng. 12, 709–722.

Baek, S.-H., Byun, H.-S., 2016. Bubble-point measurement for the binary mixture of propargyl acrylate and propargyl methacrylate in supercritical carbon dioxide. J. Chem. Thermodyn. 92, 191–197. https://doi.org/10.1016/j.jct.2015.09.014.

Balbinot Filho, C.A., Dias, J.L., Rebelatto, E.A., Lanza, M., 2023. High-pressure phase equilibrium data of carbon dioxide/food-relevant systems (2011–2022): experimental methods, multiphase behavior, thermodynamic modeling, and applications. Fluid Phase Equilib. 572,. https://doi.org/10.1016/j.fluid.2023.113851 113851.

Bhawangirkar, D.R., Adhikari, J., Sangwai, J.S., 2018. Thermodynamic modeling of phase equilibria of clathrate hydrates formed from CH4, CO2, C2H6, N2 and C3H8, with different equations of state. J. Chem. Thermodynamics. 117, 180–192.

Bolm, C., Beckmann, O., Dabard, O.A.G., 1999. The search for new environmentally friendly chemical processes. Angew. Chem. Int. Ed. 38, 907–909. https://doi.org/10.1002/(SICI)1521-3773(19990401)38:7<907::AID-ANIE907>3.0.CO;2-%23.

Braga, M.E.M., Gaspar, M.C., de Sousa, H.C., 2023. Supercritical fluid technology for agrifood materials processing. Curr. Opin. Food Sci. 50,. https://doi.org/10.1016/j.cofs.2022.100983 100983.

Braunschmid, H., Guilhot, R., Dötterl, S., 2021. Floral scent and pollinators of cypripedium calceolus L. at different latitudes. Diversity 13, 5. https://doi.org/10.3390/d13010005.

butyl acetoacetate, 591-60-6, n.d. http://www.thegoodscentscompany.com/data/rw1013081.html (accessed May 5, 2023).

Buy Hexyl acetoacetate – 13562-84-0 | BenchChem, n.d. https://www.benchchem.com/product/b078972 (accessed September 18, 2023).

Buy Octyl acetoacetate – 16436-00-3 | BenchChem, n.d. https://www.benchchem.com/product/b098030 (accessed September 18, 2023).

Calvo-Flores, F.G., Monteagudo-Arrebola, M.J., Dobado, J.A., Isac-García, J., 2018. Green and bio-based solvents, Top Curr. Chem (Z). 376, 18. https://doi.org/10.1007/s41061-018-0191-6.

Dhamodharan, D., Lee, C.-W., Byun, H.-S., 2023. High-pressure phase equilibrium of the binary systems CO2 + 355-TMHA and CO2 + 335-TMCHMA. New J. Chem. 47, 4043–4051. https://doi.org/10.1039/D2NJ05825A.

FH60066 | 13562-84-0 | Hexyl Acetoacetate | Biosynth, n.d. https://www.biosynth.com/p/FH60066/13562-84-0-hexyl-acetoacetate (accessed September 18, 2023).

Gao, Y., Li, C., Xia, S., Ma, P., 2020. Estimation and correlation of phase equilibrium of CO2–hydrocarbon systems with PRMHV2-UNIFAC and PRMHV2-NRTL models. J. Chem. Eng. Data. 65, 655–663. https://doi.org/10.1021/acs.jced.9b00890.

Gao, Y., Li, C., Xia, S., Ma, P., 2021. The solubility of CO2 in (hexane + cyclohexane) and (cyclopentane + ethylbenzene) and (toluene + undecane) systems at high pressures. J. Chem. Thermodyn. 154,. https://doi.org/10.1016/j.jct.2020.106324 106324.

Ghoderao, P.N.P., Dalvi, V.H., Narayan, M., 2018. A four-parameter cubic equation of state for pure compounds and mixtures. Chem. Eng. Sci. 190, 173–189.

Ghoderao, P.N.P., Dalvi, V.H., Narayan, M., 2019. A four parameter cubic equation of state with temperature dependent covolume parameter. Chin. J. Chem. Eng. 27, 1132–1148. https://doi.org/10.1016/j.cjche.2018.08.013.

Ghoderao, P.N.P., Dalvi, V.H., Narayan, M., 2019. A five-parameter cubic equation of state for pure fluids and mixtures. Chem. Eng. Sci.: X. 3,. https://doi.org/10.1016/j.cesx.2019.100026 100026.

Ghoderao, P.N.P., Lee, C.-W., Byun, H.-S., 2023. Phase behavior for the poly(2-ethyl-2-oxazoline) + supercritical DME + alcohol and carbon dioxide + 2-ethyl-2-oxazoline mixtures at high pressure. Chem. Eng. Sci. 270,. https://doi.org/10.1016/j.ces.2023.118566 118566.

Ghoderao, P.N.P., Lee, C.-W., Byun, H.-S., 2023. Phase behavior investigation of the vinyl toluene and poly (vinyl toluene) + co-solvents in supercritical CO2. J. Ind. Eng. Chem. 121, 92–99. https://doi.org/10.1016/j.jiec.2023.01.010.

Giles, J.E., Woodwell, R.G., 1998. 8 - Precision Cleaning With Supercritical Fluid: A Case Study. In: McHardy, J., Sawan, S.P. (Eds.), Supercritical Fluid Cleaning. William Andrew Publishing, Westwood, NJ, pp. 195–219. https://doi.org/10.1016/B978-081551416-9.50010-0.

Girardi, D.G.L., Letsch, A.L., Rebelatto, E.A., Mayer, D.A., de Oliveira, J.V., 2023. High pressure phase behavior and thermodynamic modeling of the carbon dioxide + chloroform + globalide system. Fluid Phase Equilib. 572,. https://doi.org/10.1016/j.fluid.2023.113831 113831.

Joshi, A., Mekala, P., Sangwai, J.S., 2012. Modeling phase equilibria of semiclathrate hydrates of CH4, CO2 and N2 in aqueous solution of tetra-n-butyl ammonium bromide. J. Nat. Gas Chem. 21, 459–465.

Khalil, Y.F., 2019. Sustainability assessment of solvolysis using supercritical fluids for carbon fiber reinforced polymers waste management. Sustain. Prod. Consum. 17, 74–84. https://doi.org/10.1016/j.spc.2018.09.009.

Knez, Ž., Markočič, E., Leitgeb, M., Primožič, M., Knez Hrnčič, M., Škerget, M., 2014. Industrial applications of supercritical fluids: A review. Energy 77, 235–243. https://doi.org/10.1016/j.energy.2014.07.044.

Kohli, R., 2019. Chapter 6 - Applications of Supercritical Carbon Dioxide for Removal of Surface Contaminants. In: Kohli, R., Mittal, K.L. (Eds.), Developments in Surface Contamination and Cleaning: Applications of Cleaning Techniques. Elsevier, pp. 209–249. https://doi.org/10.1016/B978-0-12-815577-6.00006-2.

Kristanto, T., Tiwikrama, A.H., Lee, M.-J., 2023. Vapor-liquid equilibrium phase behavior of binary systems of carbon dioxide with dimethyl adipate or monomethyl adipate. J. Supercrit. Fluids 194,. https://doi.org/10.1016/j.supflu.2023.105856 105856.

Lee, H.-S., Ghoderao, P.N.P., Soo Park, M., Byun, H.-S., 2023. Phase equilibria for the two-component systems of allyl acetoacetate, methyl acetoacetate and ethyl acetoacetate under high-pressure CO2. J. Mol. Liq. 387,. https://doi.org/10.1016/j.molliq.2023.122651 122651.

Li, C., Gao, Y., Xia, S., Shang, Q., Ma, P., 2019. Calculation of the Phase Equilibrium of CO2–Hydrocarbon Binary Mixtures by PR-BM EOS and PR EOS. Trans. Tianjin Univ. 25, 540–548. https://doi.org/10.1007/s12209-019-00194-y.

Li, K., Xu, Z., 2019. A review of current progress of supercritical fluid technologies for e-waste treatment. J. Clean. Prod. 227, 794–809. https://doi.org/10.1016/j.jclepro.2019.04.104.

Liang, B., Hao, J., Zhu, N., Han, L., Song, L., Hong, H., 2023. Formulation of nitrendipine/hydroxypropyl-β-cyclodextrin inclusion complex as a drug delivery system to enhance the solubility and bioavailability by supercritical fluid technology. Eur. Polym. J. 187,. https://doi.org/10.1016/j.eurpolymj.2023.111880 111880.

Liu, Z., Navik, R., Tan, H., Xiang, Q., Wahyudiono, M., Goto, R.M., Ibarra, Y.Z., 2022. Graphene-based materials prepared by supercritical fluid technology and its application in energy storage. J. Supercrit. Fluids. 188,. https://doi.org/10.1016/j.supflu.2022.105672 105672.

López-Hortas, L., Rodríguez, P., Díaz-Reinoso, B., Gaspar, M.C., de Sousa, H.C., Braga, M.E.M., Domínguez, H., 2022. Supercritical fluid extraction as a suitable technology to recover bioactive compounds from flowers. J. Supercrit. Fluids. 188,. https://doi.org/10.1016/j.supflu.2022.105652 105652.

Manjare, S.D., Dhingra, K., 2019. Supercritical fluids in separation and purification: a review. Mater. Sci. Energy Technol. 2, 463–484. https://doi.org/10.1016/j.mset.2019.04.005.

Np Ghoderao, P., Lee, C.-W., Byun, H.-S., 2023. Binary systems for the trimethylolpropane triacrylate and trimethylolpropane trimethacrylate in supercritical carbon dioxide: experiment and modeling. J. Mol. Liq. 372,. https://doi.org/10.1016/j.molliq.2023.121206 121206.

Okolie, J.A., Nanda, S., Dalai, A.K., Kozinski, J.A., 2022. Chapter 9 - Advances in the industrial applications of supercritical carbon dioxide. In: Nanda, S., Vo, D.-V.N., Nguyen, V.-H. (Eds.), Carbon Dioxide Capture and Conversion. Elsevier, pp. 237–256. https://doi.org/10.1016/B978-0-323-85585-3.00008-0.

Poling, B.E., Prausnitz, J.M., O'Connell, J.P., 2001. The Properties of Gases and Liquids. McGraw-Hill, New York.

Preetam, A., Jadhao, P.R., Naik, S.N., Pant, K.K., Kumar, V., 2023. Supercritical fluid technology – an eco-friendly approach for resource recovery from e-waste and plastic waste: a review. Sep. Purif. Technol. 304,. https://doi.org/10.1016/j.seppur.2022.122314 122314.

PubChem, Butyl acetoacetate, n.d. https://pubchem.ncbi.nlm.nih.gov/compound/11576 (accessed May 5, 2023).

Ramsey, E., Sun, Q., Zhang, Z., Zhang, C., Gou, W., 2009. Mini-review: green sustainable processes using supercritical fluid carbon dioxide. J. Environ. Sci. 21, 720–726.

Reid, R.C., Prausnitz, J.M., Poling, B.E., 1987. The Properties of Gases & Liquids. McGraw-Hill Inc, New York.

Senyay-Oncel, D., Kimiz-Gebologlu, I., Yesil-Celiktas, O., 2023. New developments in supercritical fluids as a green technology: Processing of β-glucanase with sub- and supercritical carbon dioxide. Biochem. Eng. J. 195,. https://doi.org/10.1016/j.bej.2023.108934 108934.

Sodeifian, G., Arbab Nooshabadi, M., Razmimanesh, F., Tabibzadeh, A., 2023. Solubility of buprenorphine hydrochloride in supercritical carbon dioxide: study on experimental measuring and thermodynamic modeling. Arab. J. Chem. 16,. https://doi.org/10.1016/j.arabjc.2023.105196 105196.

Tabernero, A., González-Garcinuño, Á., Cardea, S., Martín del Valle, E., 2022. Supercritical carbon dioxide and biomedicine: opening the doors towards biocompatibility. Chem. Eng. J. 444,. https://doi.org/10.1016/j.cej.2022.136615 136615.

Tran, P., Park, J.-S., 2021. Application of supercritical fluid technology for solid dispersion to enhance solubility and bioavailability of poorly water-soluble drugs. Int. J. Pharm. 610,. https://doi.org/10.1016/j.ijpharm.2021.121247 121247.

Tsai, W.-C., Wang, Y., 2019. Progress of supercritical fluid technology in polymerization and its applications in biomedical engineering. Prog. Polym. Sci. 98,. https://doi.org/10.1016/j.progpolymsci.2019.101161 101161.

Tsoka, C., Johns, W.R., Linke, P., Kokossis, A., 2004. Towards sustainability and green chemical engineering: tools and technology requirements. Green Chem. 6, 401–406. https://doi.org/10.1039/B402799J.

Wagare, D.S., Shirsath, S.E., Shaikh, M., Netankar, P., 2021. Sustainable solvents in chemical synthesis: a review. Environ. Chem. Lett. 19, 3263–3282.

Yang, B., Wang, H.-Z., Li, G.-S., Wang, B., Chang, L., Tian, G.-H., Zhao, C.-M., Zheng, Y., 2022. Fundamental study and utilization on supercritical CO2 fracturing developing unconventional resources: current status, challenge and future perspectives. Pet. Sci. 19, 2757–2780. https://doi.org/10.1016/j.petsci.2022.08.029.

Zhang, X., Heinonen, S., Levänen, E., 2014. Applications of supercritical carbon dioxide in materials processing and synthesis. RSC Adv. 4, 61137–61152. https://doi.org/10.1039/C4RA10662H.